Local structure and dynamics in methylammonium, formamidinium and cesium tin(II) mixed-halide perovskites from ^{119}Sn solid-state NMR

Dominik J. Kubicki,[a,b] Daniel Prochowicz,[d] Elodie Salager,[f,g] Aydar Rakhmatullin,[f] Clare P. Grey*[b], Lyndon Emsley*[c], Samuel Stranks*[a]

[a]*Cavendish Laboratory, Department of Physics, University of Cambridge, JJ Thomson Avenue, Cambridge, CB3 0HE, UK*
[b]*Department of Chemistry, University of Cambridge, Lensfield Road, Cambridge, CB2 1EW, UK*
[c]*Laboratory of Magnetic Resonance, Institute of Chemical Sciences and Engineering, Ecole Polytechnique Fédérale de Lausanne (EPFL), CH-1015 Lausanne, Switzerland*
[d]*Institute of Physical Chemistry, Polish Academy of Sciences, Kasprzaka 44/52, 01-224 Warsaw, Poland*
[e]*Laboratory of Photonics and Interfaces, Institute of Chemical Sciences and Engineering, Ecole Polytechnique Fédérale de Lausanne (EPFL), CH-1015 Lausanne, Switzerland*
[f]*Conditions Extrêmes et Matériaux: Haute Température et Irradiation (CEMHTI), UPR 3079 CNRS, Université d'Orléans, 1D Avenue de la Recherche Scientifique, Orléans 45071, France*
[g]*Réseau sur le Stockage Electrochimique de l'Energie (RS2E), FR 3459 CNRS, 33 Rue Saint Leu, Amiens 80039, France*

Table of contents

List of figures and tables

Synthesis of the materials

$MASnCl_6$: MACl (68 mg, 1.00 mmol), $SnCl_2$ (190 mg, 1.00 mmol),
$MASnBr_3$: MABr (112 mg, 1.00 mmol), $SnBr_2$ (279 mg, 1.00 mmol),
$MASnI_3$: MAI (159 mg, 1.00 mmol), SnI_2 (373 mg, 1.00 mmol),

$MASnCl_{2.7}Br_{0.3}$: MACl (61 mg, 0.9 mmol), MABr (11 mg, 0.1 mmol), $SnCl_2$ (171 mg, 0.9 mmol), $SnBr_2$ (28 mg, 0.1 mmol)
$MASnCl_{2.1}Br_{0.9}$: MACl (47 mg, 0.7 mmol), MABr (34 mg, 0.3 mmol), $SnCl_2$ (133 mg, 0.7 mmol), $SnBr_2$ (84 mg, 0.3 mmol)
$MASnCl_{1.5}Br_{1.5}$: MACl (34 mg, 0.5 mmol), MABr (56 mg, 0.5 mmol), $SnCl_2$ (95 mg, 0.5 mmol), $SnBr_2$ (139 mg, 0.5 mmol)

$MASnCl_{2.7}I_{0.3}$: MACl (61 mg, 0.9 mmol), MAI (16 mg, 0.1 mmol), $SnCl_2$ (171 mg, 0.9 mmol), SnI_2 (37 mg, 0.1 mmol)

$MASnBr_{0.9}I_{2.1}$: MABr (34 mg, 0.3 mmol), MAI (111 mg, 0.7 mmol), $SnBr_2$ (84 mg, 0.3 mmol), SnI_2 (261 mg, 0.7 mmol)
$MASnBr_{1.5}I_{1.5}$: MABr (56 mg, 0.5 mmol), MAI (79 mg, 0.5 mmol), $SnBr_2$ (139 mg, 0.5 mmol), SnI_2 (186 mg, 0.5 mmol)
$MASnBr_{2.1}I_{0.9}$: MABr (78 mg, 0.7 mmol), MAI (48 mg, 0.3 mmol), $SnBr_2$ (195 mg, 0.7 mmol), SnI_2 (112 mg, 0.3 mmol)
$MASnBr_{2.55}I_{0.45}$: MABr (95 mg, 0.85 mmol), MAI (24 mg, 0.25 mmol), $SnBr_2$ (237 mg, 0.85 mmol), SnI_2 (56 mg, 0.25 mmol)
$MASnBr_{2.7}I_{0.3}$: MABr (101 mg, 0.9 mmol), MAI (16 mg, 0.1 mmol), $SnBr_2$ (251 mg, 0.9 mmol), SnI_2 (37 mg, 0.1 mmol)

MA_2SnBr_6: MABr (224 mg, 2.00 mmol), $SnBr_4$ (438 mg, 1.00 mmol),
MA_2SnI_6: MAI (318 mg, 2.00 mmol), SnI_4 (626 mg, 1.00 mmol),

$FASnI_3$: FAI (172 mg, 1.00 mmol), SnI_2 (373 mg, 1.00 mmol),
$FASnBr_3$: FABr (125 mg, 1.00 mmol), $SnBr_2$ (279 mg, 1.00 mmol),
$FASnCl_3$: FACl (81 mg, 1.00 mmol), $SnCl_2$ (190 mg, 1.00 mmol),
$MA_{0.5}FA_{0.5}SnBr_3$: MABr (56 mg, 0.5 mmol), FABr (62 mg, 0.5 mmol), $SnBr_2$ (279 mg, 1.00 mmol),
$MA_{0.5}FA_{0.5}SnCl_3$: MACl (34 mg, 0.5 mmol), FACl (40 mg, 0.5 mmol), $SnCl_2$ (190 mg, 1.00 mmol),
$CsSnI_3$: CsI (260 mg, 1.00 mmol), SnI_2 (373 mg, 1.00 mmol),
$CsSnBr_3$: CsBr (213 mg, 1.00 mmol), $SnBr_2$ (279 mg, 1.00 mmol),
$CsSnCl_3$: CsCl (168 mg, 1.00 mmol), $SnCl_2$ (190 mg, 1.00 mmol),
$CsSnCl_{1.5}Br_{1.5}$: CsCl (168 mg, 1.00 mmol), $SnCl_2$ (95 mg, 0.5 mmol), $SnBr_2$ (139 mg, 0.5 mmol),

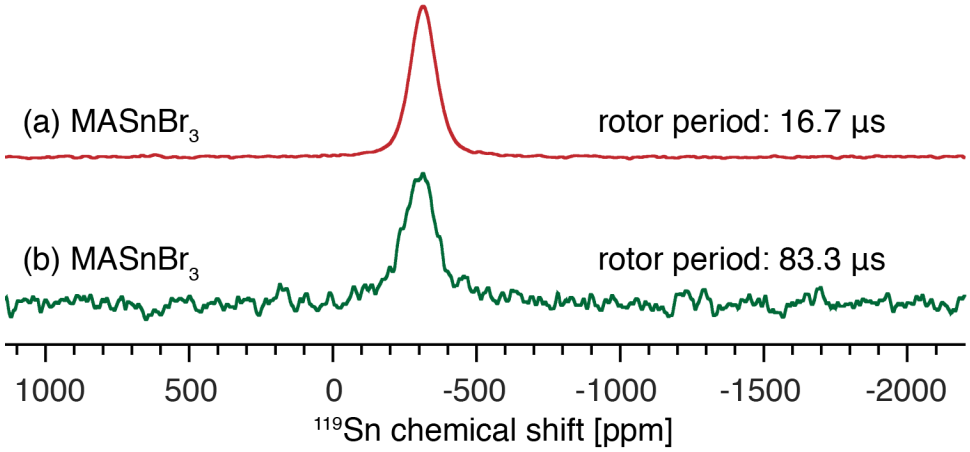

Figure S1. Echo-detected ^{119}Sn MAS NMR spectra of $MASnBr_3$ at 4.7 T, 298 K and 12 kHz MAS using a refocusing echo period of (a) 16.7 µs (asynchronous), (b) 83.3 µs (rotor synchronized). The rotor-synchronized echo period does not lead to the appearance of spinning sidebands and its only effect is lower signal intensity due to fast transverse relaxation. Number of scans: (a) 1024, (b) 4096. Recycle delay: 50 ms.

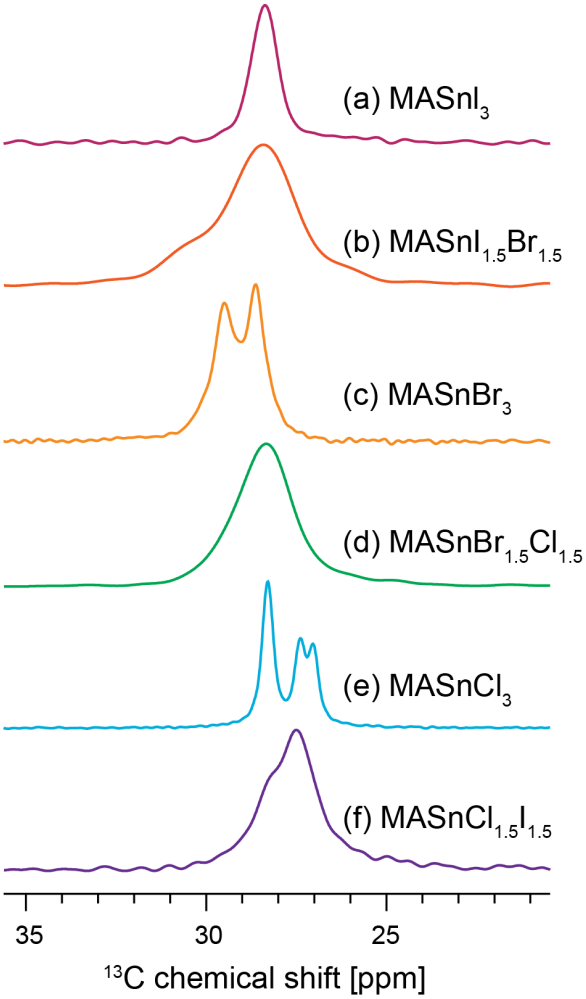

Figure S2. ^{1}H-^{13}C CP MAS NMR spectra at 11.7 T, 100 K and 12 kHz MAS of (a) $MASnI_3$, (b) $MASnI_{1.5}Br_{1.5}$, (c) $MASnBr_3$, (d) $MASnBr_{1.5}Cl_{1.5}$,(e) $MASnCl_3$, (f) $MASnCl_{1.5}I_{1.5}$. The well-resolved features in panels c and e correspond to distinct MA environments present in the low-symmetry low temperature phases of $MASnBr_3$ and $MASnCl_3$, respectively. The spectra

of mixed-halide compositions are broader as compared to the single halide materials, consistent with the presence of halide disorder. Recycle delay: 2 s. Number of scans: 256-1024. ^{1}H decoupling: 100 kHz (SPINAL-64). Contact time: 1 ms.

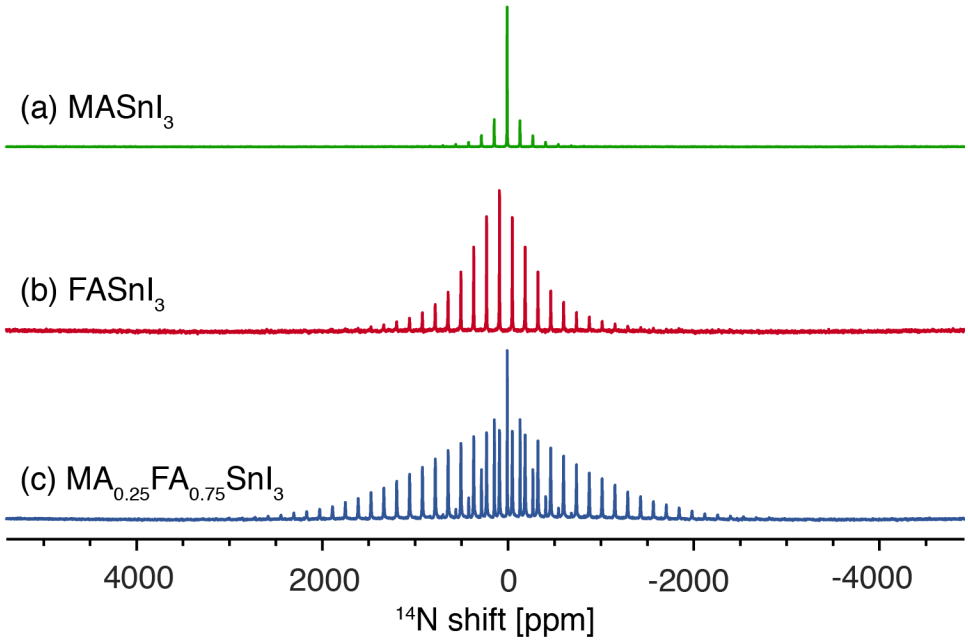

Figure S3. ^{14}N MAS NMR echo-detected spectra at 11.7 T, 298 K and 5 kHz MAS of (a) $MASnI_3$, (b) $FASnI_3$, (c) $MA_{0.25}FA_{0.75}SnI_3$. The broadening of the spinning sideband manifold in the mixed-cation case (panel c) is indicative of lowering of the cubooctahedral symmetry. Recycle delay: 0.3 s. RF strength: 62.5 kHz.

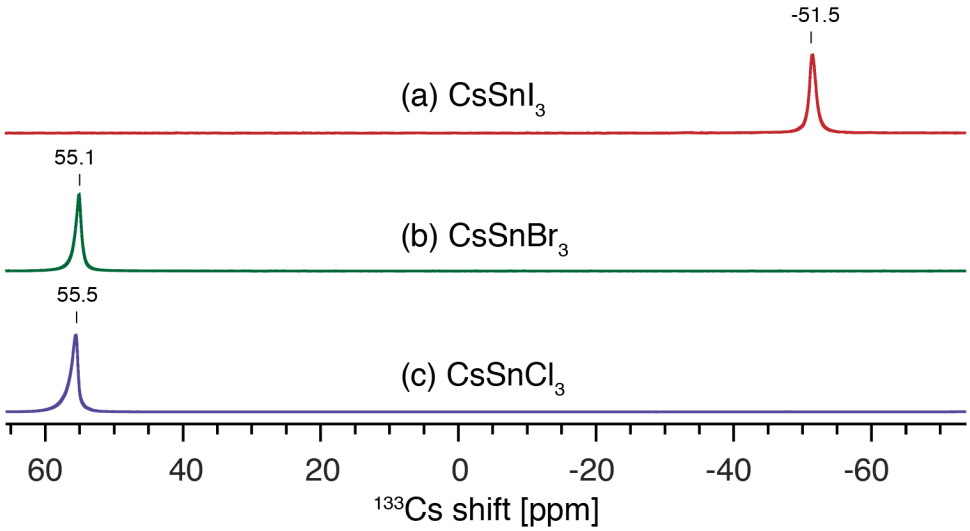

Figure S4. ^{133}Cs MAS NMR echo-detected spectra at 16.4 T, 298 K and 12 kHz MAS of (a) $CsSnI_3$, (b) $CsSnBr_3$, (c) $CsSnCl_3$. The similarity of ^{133}Cs shift of $CsSnBr_3$ and $CsSnCl_3$ is coincidental as the compounds are cubic and monoclinic at room temperature, respectively. ^{133}Cs resonances in 3D halide perovskites have been shown to be strongly temperature dependent and an upfield shift (to lower ppm values) is expected on increasing the temperature and symmetry in $CsSnCl_3$, consistent with previous reports.[1,2] Recycle delay: (a) 120 s, (b) 40 s, (c) 40 s. RF strength: 27.8 kHz.

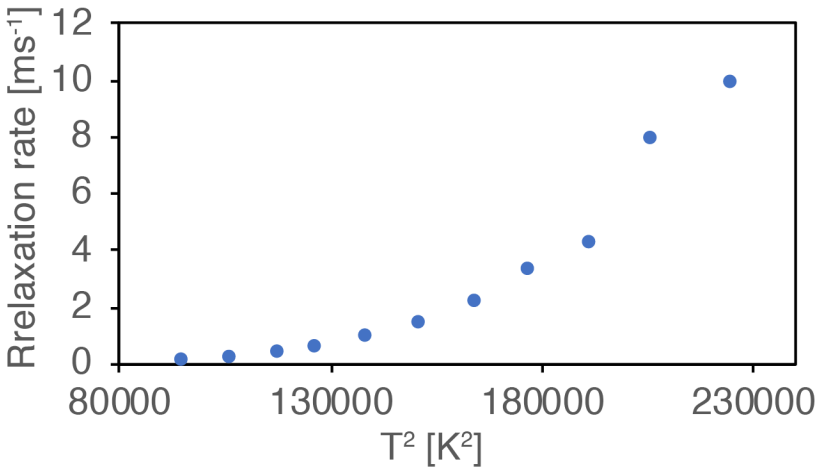

Figure S5. A plot of the relaxation rate R (R=1/T_1) of the variable-temperature T_1 relaxation data for $MASnBr_3$ at 16.4 T as a function of the square of temperature. The dependence would be linear if relaxation was dominated by spin-phonon Raman scattering.[3]

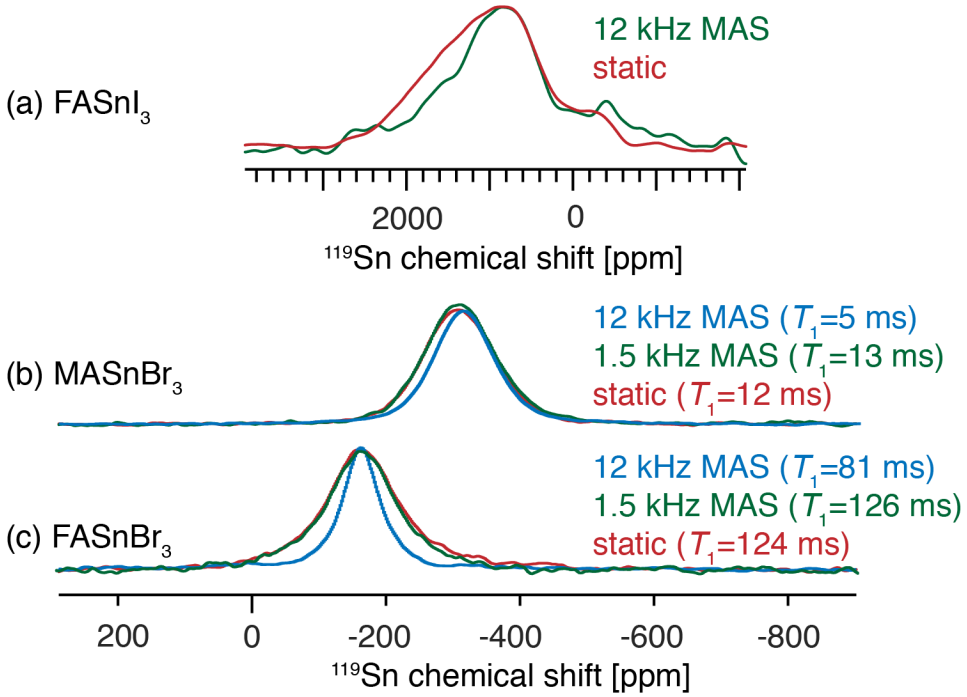

Figure S6. The effect of spinning on ^{119}Sn NMR spectra and T_1 relaxation of tin(II) halide perovskites: (a) $FASnI_3$ (red: static, green: 12 kHz MAS), (b) $MASnBr_3$ (red: static, green 1.5 kHz MAS, blue: 12 kHz MAS), (c) $FASnBr_3$ (red: static, green: 1.5 kHz MAS). The use of MAS does not lead to shortening of the T_1 which excludes MAS-induced heteronuclear polarization exchange as a possible relaxation mechanism in $MASnBr_3$. The slight shortening of T_1 on going from 1.5 to 12 kHz (panel b) is a temperature-induced effect.

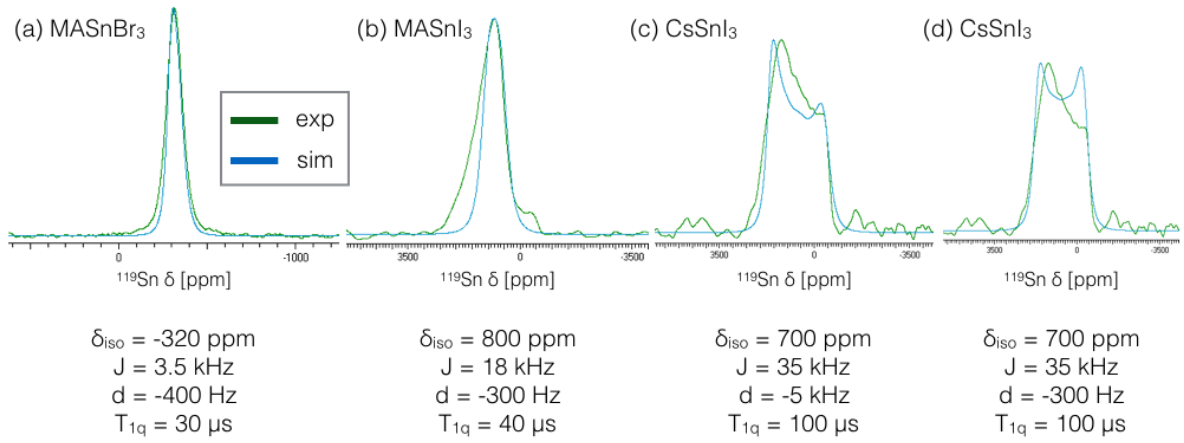

Figure S7. WSolids1 (*WSolids1 ver. 1.21.3, K. Eichele, Universität Tübingen, 2015*) line shape simulations in the extreme narrowing regime of (a) $MASnBr_3$, (b) $MASnI_3$, (c,d) $CsSnI_3$. The relevant simulation parameters are given below the spectra. exp – experimental spectrum, sim – simulated spectrum, J – ^{119}Sn-X J-coupling, d – ^{119}Sn-X dipole coupling, T_{1q} – estimated T_1 relaxation of the quadrupolar nucleus. Dipolar couplings expected based on the crystal structures (Sn-X distance = 2.9-3.1 Å) are as follows: ^{119}Sn-^{81}Br: d = -410 Hz, ^{119}Sn-^{79}Br: d = -380 Hz, ^{119}Sn-^{127}I: d = -304 Hz. The width of the spectrum is largely determined by the magnitude of J while d introduces a small asymmetry and T_{1q} determines the line broadening in the extreme narrowing regime. In the case of $CsSnI_3$, the asymmetry is reproduced well with a d value larger than the coupling expected based on the crystal structure (panel c). Using the coupling strength based on the crystal structure leads to a more symmetric simulated spectrum (panel d). Since the spectra are echo-acquired, we expect that the slight asymmetry may be an artifact caused by anisotropic ^{119}Sn T_2 relaxation.

Supplementary Note 1

It is worth noting that the CSA patterns of $MASnCl_{1.5}Br_{1.5}$ (fig. 2f) and $MASnBr_{2.55}I_{0.45}$ (fig. 3g) yield a single ^{119}Sn peak while a sizeable CSA is expected in these cases due to asymmetric coordination of the tin(II) site. Taking a typical value of ^{119}Sn CSA spanning 100 kHz, the dynamic process which leads to its averaging has to occur at a faster rate, *i.e.* with a correlation time shorter than 1/(100 kHz) = 10 μs. Since the previously determined halide hopping rates (>0.1 GHz) correspond to correlation times <10 ns, halide hopping might be the source of CSA averaging.

Supplementary Note 2

Estimation of the ^{119}Sn T_1 minimum in the dipole-dipole relaxation mechanism for ^{119}Sn coupled to ^{79}Br at 4.7 T:

$$\frac{1}{T_1} = \frac{4}{30}\left(\frac{\mu_0}{4\pi}\right)^2 \frac{\gamma_{Sn}^2 \gamma_{Br}^2 \hbar}{r^6} S(S+1)$$
$$\left(\frac{\tau}{1+(\omega_{Sn}-\omega_{Br})^2\tau^2} + \frac{3\tau}{1+{\omega_{Sn}}^2\tau^2} + \frac{6\tau}{1+(\omega_{Sn}+\omega_{Br})^2\tau^2}\right)$$

where:
permeability of free space, μ_0 – $4\pi \cdot 10^{-7}$ V·s/(A·m)
Planck constant, $\hbar$ – $1.054 \cdot 10^{-34}$ J·s
^{119}Sn gyromagnetic ratio, γ_{Sn} – $-10.03170 \cdot 10^{7}$ rad/(T·s)
^{79}Br gyromagnetic ratio, γ_{Br} – $6.72562 \cdot 10^{7}$ rad/(T·s)
^{119}Sn-^{79}Br distance in the crystal structure, r – 2.945 Å = $2.945 \cdot 10^{-10}$ m
^{119}Sn Larmor frequency, ω_{Sn} – $74.581 \cdot 10^{6}$ Hz
^{79}Br Larmor frequency, ω_{Br} – $50.108 \cdot 10^{6}$ Hz
spin of ^{79}Br, S = 3/2
correlation time, τ – an adjustable parameter
A T_1 minimum of 4.8 s is obtained for τ=13 ns.

Putting ^{81}Br gyromagnetic ratio, γ_{Br} – $7.24978 \cdot 10^{7}$ rad/(T·s) and ^{81}Br Larmor frequency, ω_{Br} – $54.0 \cdot 10^{6}$ Hz, one obtains a T_1 minimum of 4.2 s for τ=13 ns.

Supplementary Note 3

The following considerations have been used to distinguish between scalar relaxation of the first and second kind:

If the system is in the extreme narrowing limit for the $^{79/81}$Br T_{1Q}, as the temperature increases:

(i) $^{79/81}$Br T_{1Q} gets longer, ^{119}Sn T_2 gets shorter (since the flipping of the quadrupole partner gets slower).

(ii) Exchange due to halide hopping gets faster. ^{119}Sn T_2 gets longer (since the hopping of the quadrupole partner gets faster)

If the system is in the slow motion limit for the $^{79/81}$Br T_{1Q}, as the temperature increases:

(i) $^{79/81}$Br T_{1Q} gets shorter, ^{119}Sn T_2 gets longer (since the flipping of the quadrupole partner gets faster).

(ii) Exchange due to halide hopping gets faster. ^{119}Sn T_2 gets longer (since the hopping of the quadrupole partner gets faster)

It is therefore only possible to distinguish between scalar relaxation of the first and second kind based on ^{119}Sn line widths if the system is in the extreme narrowing limit. While variable-temperature relaxation measurements of $^{79/81}$Br T_{1Q} are impractical due to a very large quadrupole coupling constant in $MASnBr_3$, we corroborate that ^{119}Sn T_1 is determined by halide hopping (scalar relaxation of the first kind) based on the resulting activation energy:

1. The activation energy obtained from variable-temperature ^{119}Sn T_1 measurements matches well that from electrical measurements (Table 1 in the main text). The

thermally activated process which is being probed is therefore halide hopping. This confirms that relaxation is driven by halide hopping (i.e. scalar, 1st kind).

2. Scalar relaxation of the second kind would lead to an activation energy of the process which drives $^{79/81}$Br T_{1Q}, which is typically a Raman process related to lattice modes. Since Raman and phonon spectra fall in the far infrared to THz range, the activation energies corresponding to those processes are <0.03 eV, i.e. an order of magnitude less than what is found experimentally.

Details of NMR measurements

Table S1. Chemical shifts and peak widths of the multi-field variable-temperature T_1 relaxation data of $MASnBr_3$, measured using a saturation recovery sequence and a Hahn echo in the quasi-static regime: total echo duration 40 μs at 17.6 and 4.7 T, and 66.7 μs at 9.4 T. The uncertainties of the monoexponential T_1 fit are <1 %.

Magnetic field strength: 17.6 T

Temperature [K]	^{119}Sn chemical shift [ppm]	fwhm [kHz]	T_1 [ms]
308	-315	10.7	9.66
326	-312	10.9	5.47
343	-310	9.5	2.95
356	-306	8.6	1.87
372	-302	7.8	1.12
389	-298	6.6	0.706
405	-293	5.6	0.465
421	-287	5.8	0.305
438	-281	5.9	0.235
454	-275	7.0	0.127
474	-267	6.8	0.101
490	-266	9.9	n.d. (decomposition)

Magnetic field strength: 9.4 T

Temperature	^{119}Sn chemical shift [ppm]	fwhm [kHz]	T_1 [ms]
253	-322	10.7	201
268	-324	11.6	78
286	-317	10.8	30
313	-313	10.1	10
347	-307	8.2	3.3

Magnetic field strength: 4.7 T

Temperature	^{119}Sn chemical shift [ppm]	fwhm [kHz]	T_1 [ms]
317	-334	10.5	8.271
339	-314	8.7	4.151
347	-310	7.5	2.426
360	-314	6.9	1.644
368	-310	6.1	1.138
382	-306	4.7	0.653

393	-302	3.9	0.442
405	-300	4.2	0.329
418	-295	4.3	0.196
431	-291	4.3	0.133
455	-286	5.8	0.071

Table S2. An Arrhenius fit of the T_1 relaxation data (abscissa: 1/T, ordinate: ln(T_1/s)) to the equation: y= a+b·x for $MASnBr_3$. The errors of the least-squares fit are given as one standard deviation. The error of the average is given as one standard deviation of the average. R = 8.3144598 J/(K·mol).

magnetic field strength [T]	a	b	E_a=b·R/1000 [kJ/mol]
17.6	-18.01 ± 0.15	4165 ± 57	34.1 ± 0.5
9.4	-16.75 ± 0.41	3811 ± 12	31.8 ± 0.1
4.7	-20.74 ± 0.29	5123 ± 11	42.7 ± 0.1
		average:	36.2 ± 5.7

Table S3. ^{119}Sn T_1 values measured using a saturation-recovery sequence and fitted using a monoexponential function. The uncertainties of the fit are <1 %.

compound	^{119}Sn T_1 [s]
$MASnCl_3$	60
$MASnCl_{2.7}Br_{0.3}$	29.7
$MASnCl_{2.1}Br_{0.9}$	2.59
$MASnCl_{1.5}Br_{1.5}$	0.352
$MASnBr_3$	0.0053
$MASnBr_{2.7}I_{0.3}$	0.0011
$MASnBr_{2.1}I_{0.9}$	0.000164
$MASnI_3$	0.000545
β-Sn	0.00012
$SnCl_2$	26.4
$SnBr_2$	1.12
SnI_2	0.528
$SnBr_4$	1.95
SnI_4	11.5
MA_2SnBr_6	9.9
MA_2SnI_6	0.001

Table S4. Acquisition and processing parameters used for the spectra in the main text.

^{119}Sn spectra

composition	Figure	recycle delay [s]	number of scans	acquisition time [min]	Lorentzian apodization [Hz]
$SnCl_2$	2	34	32	18	200
$SnBr_2$		1.5	6204	155	1000
$MASnCl_3$		50	1384	1153	500
$MASnCl_{2.7}Br_{0.3}$		40	1752	1168	500

$MASnCl_{2.1}Br_{0.9}$		3	1892	95	4000
$MASnCl_{1.5}Br_{1.5}$		0.5	3900	33	1000
$MASnBr_3$		0.05	4096	3	1000
$SnBr_4$		2.5	2260	94	1000
MA_2SnBr_6		13	680	147	2000
SnI_2	3	1	2224	37	2000
$MASnI_3$		0.01	32768 ×3 offsets	16	20000
$MASnCl_{2.7}I_{0.3\ (fast)}$		0.05	55800	47	10000
$MASnCl_{2.7}I_{0.3\ (slow)}$		50	2008	1673	100
$MASnBr_{0.9}I_{2.1}$		0.01	3654026	609	10000
$MASnBr_{1.5}I_{1.5}$		0.01	142604	24	10000
$MASnBr_{2.1}I_{0.9}$		0.01	135088	23	8000
$MASnBr_{2.55}I_{0.45}$		0.001	81060	1	1000
$MASnBr_{2.7}I_{0.3}$		0.05	21940	18	2000
SnI_4		20	1832	611	2000
MA_2SnI_6		0.005	55980	5	1000
$FASnI_3$	4	0.01	31624 ×5 offsets	26	20000
$CsSnI_3$		0.001	420560 ×3 offsets	21	20000
$CsSnBr_3$		0.01	53028	9	1000
$MA_{0.5}FA_{0.5}SnBr_3$		0.015	10240	3	1000
$FASnBr_3$		0.1	2048	3	1000
$MA_{0.5}FA_{0.5}SnCl_3$		60	1240	1240	500
$FASnCl_3$		60	964	964	500
$CsSnCl_3$ (monoclinic)		60	876	876	500
$CsSnCl_3$ (cubic)		5	128	11	200
$CsSnCl_{1.5}Br_{1.5}$		0.5	3300	28	100
$MASnBr_3$ (degraded)	5	13	4972	1077	500
SnO_2		12	128	26	100
SnO_2 + 10 mol% $SnBr_2$		12	356	71	100
$FASnBr_3$ (degraded at RT)		13	4796	1039	1000
$FASnBr_3$ (degraded at 250 °C)		13	3300	715	500
$CsSnBr_3$ (degraded), perovskite region		0.01	53028	9	1000
$CsSnBr_3$ (degraded), decomposition products		13	968	210	2000
$MASnI_3$ (degraded), perovskite region		0.01	32768	5	10000
$MASnI_3$ (degraded), MA_2SnI_6 region		0.005	55980	5	1000

$MASnI_3$ (degraded), SnO_2 region		12	2280	456	1000
$MASnI_3$ (degraded), β-Sn region		0.001	12240000	965*	2000
$FASnI_3$ (degraded)		0.005	46844	4	1000
$CsSnI_3$ (degraded)		0.1	58112	97	1000
β-tin (metal)		0.01	15892	3	2000

*comprising safety delays to reduce the duty cycle of the probe (effective recycle delay of 4.7 ms)

Table S5. Summary of the degradation products of tin(II) halide perovskites detected using ^{119}Sn MAS NMR. Note that not all possible degradation products were detected for all samples - see the discussion in the main text for details.

Material	Degradation conditions	Figure in the main text	Detected degradation products
$MASnBr_3$	1 h at 250 °C in air	5b	MA_2SnBr_6, SnO_2, ($SnBr_4$)
$FASnBr_3$	5 days at RT, in air	5f	FA_2SnBr_6, SnO_2,
$FASnBr_3$	Same sample as above + 0.5 h at 250 °C in air	5g	FA_2SnBr_6, SnO_2,
$CsSnBr_3$	0.5 h at 350 °C in air	5i	Cs_2SnBr_6, SnO_2
$MASnI_3$	1 h at 150 °C in air	5k	MA_2SnI_6, SnO_2, metallic tin
$FASnI_3$	1 h at RT in air	5m	FA_2SnI_6
$CsSnI_3$	3 h at 100 °C in air	5o	Cs_2SnI_6

XRD data

Powder X-ray diffraction patterns were recorded on an X'Pert MPD PRO (Panalytical) diffractometer equipped with a ceramic tube (Cu anode, $\lambda = 1.54060$ Å), a secondary graphite (002) monochromator and an RTMS X'Celerator (Panalytical) in an angle range of $2\theta = 5°$ to 40°, by step scanning with a step of 0.02 degree.

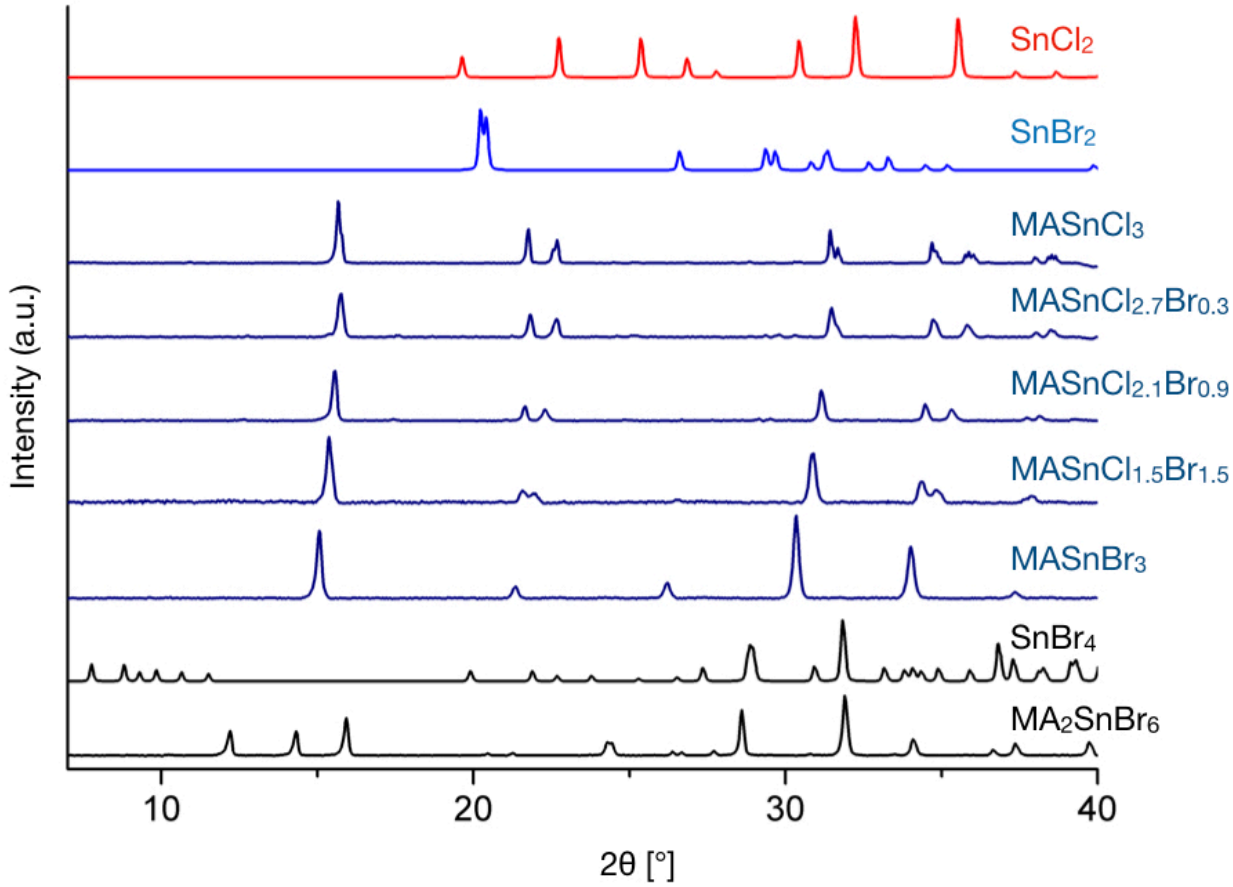

Figure S8. Powder X-ray diffraction patterns of the materials reported in Figure 2 of the main text.

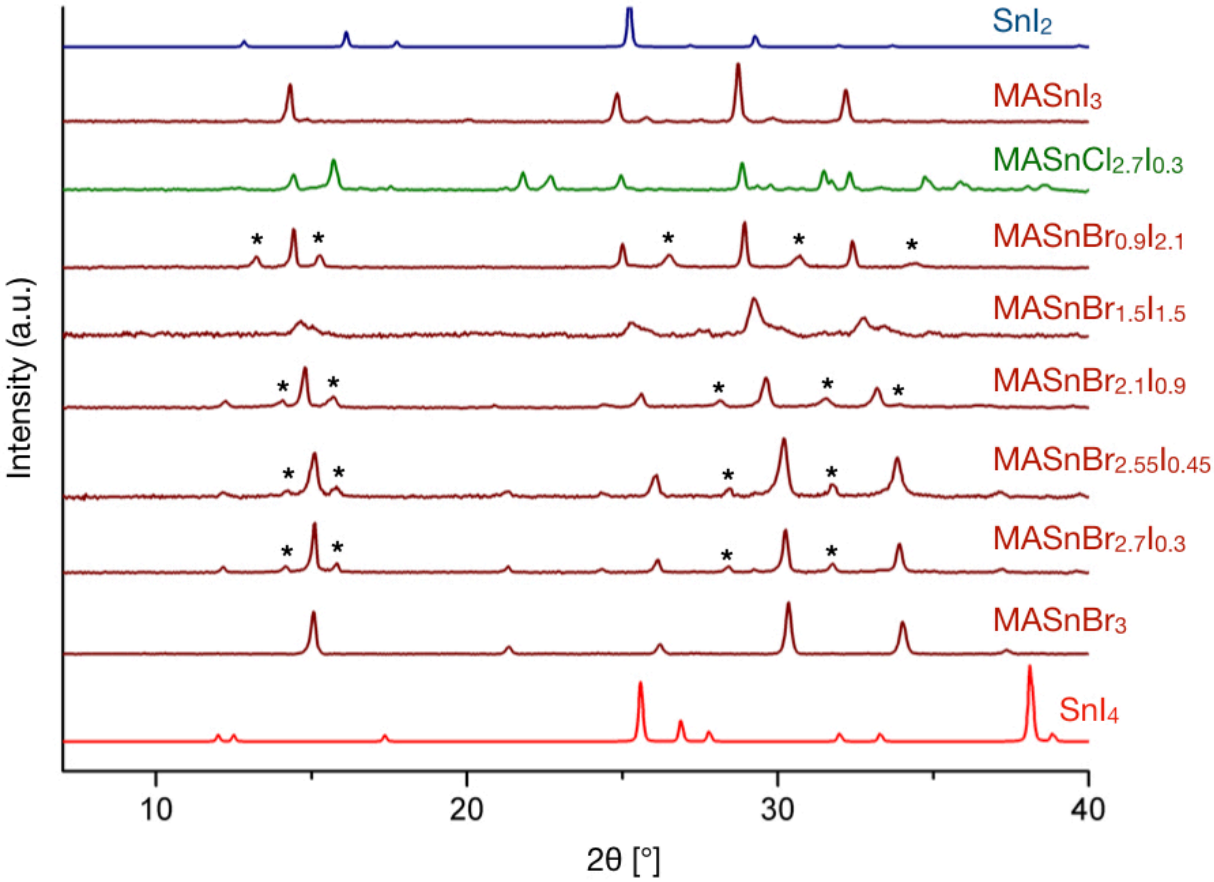

Figure S9. Powder X-ray diffraction patterns of the materials reported in Figure 3 of the main text. The asterisks indicate the corresponding oxidized A_2SnX_6 phase which slowly forms during the XRD measurement which is carried out in air.

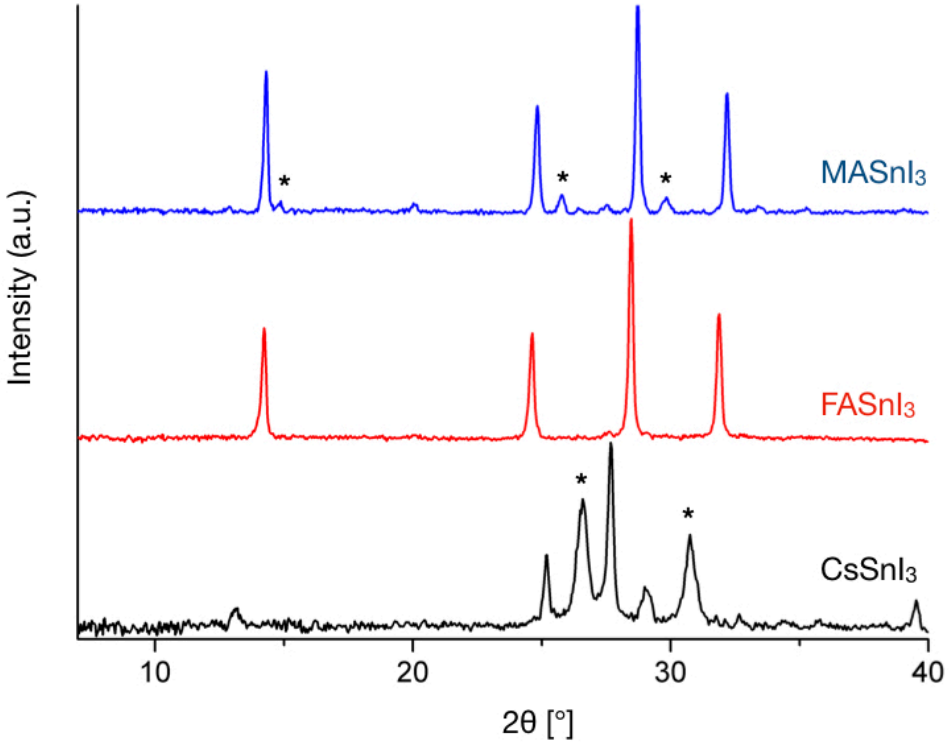

Figure S10. Powder X-ray diffraction patterns of the materials reported in Figure 4a-c of the main text. The asterisks indicate the corresponding oxidized A_2SnX_6 phase which slowly forms during the XRD measurement which is carried out in air.

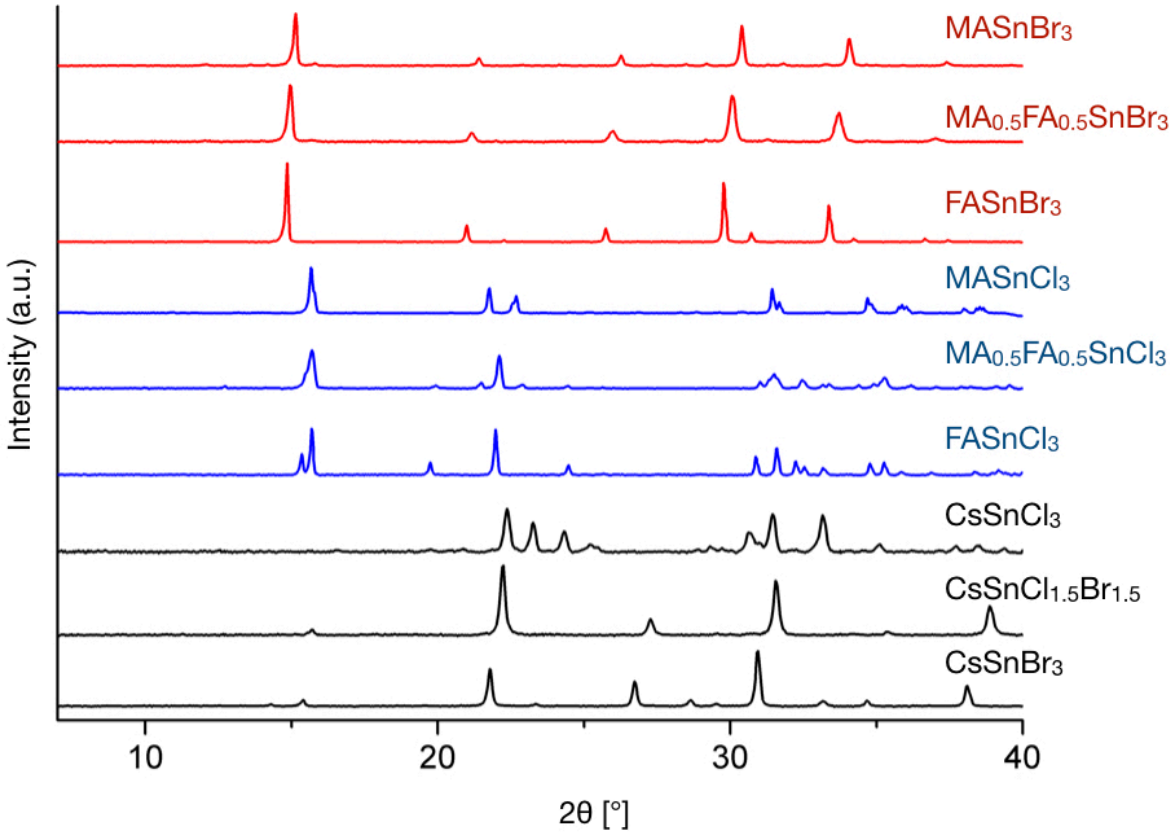

Figure S11. Powder X-ray diffraction patterns of the materials reported in Figure 4d-m of the main text.

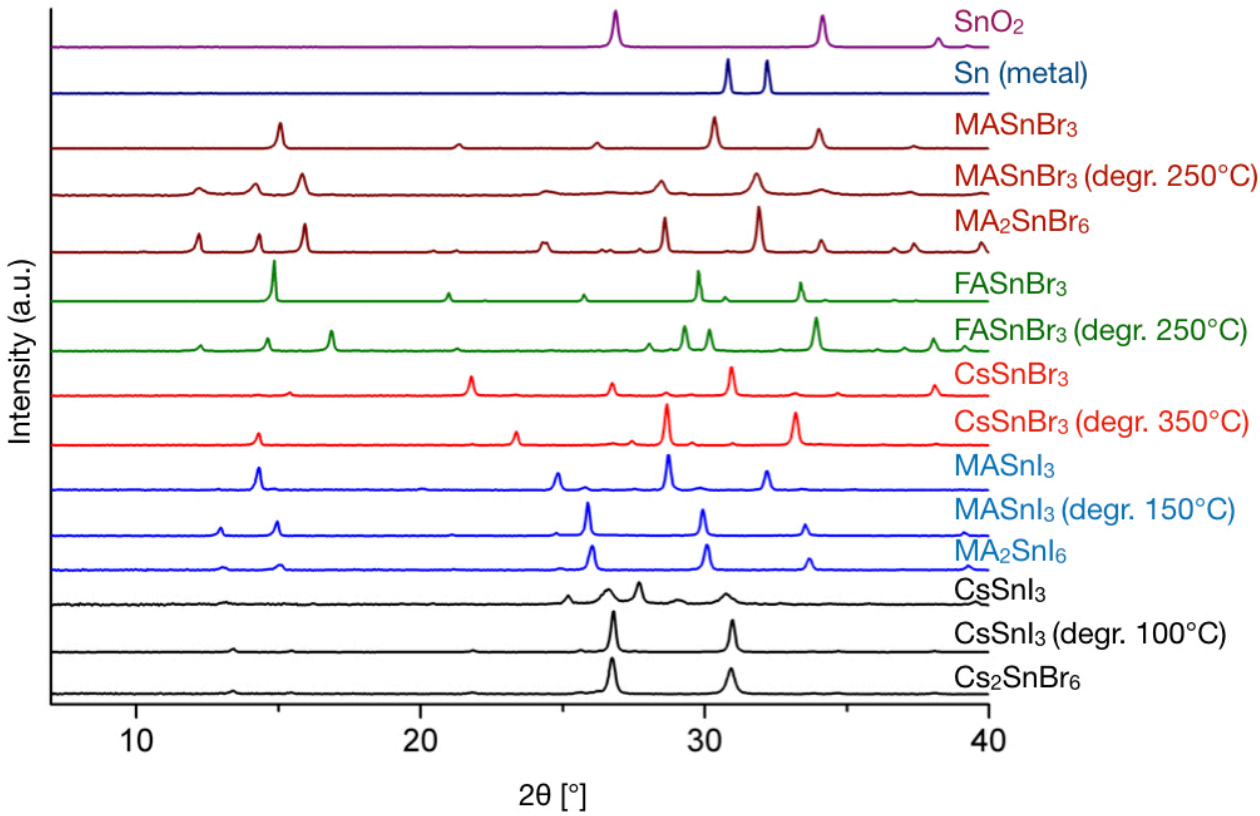

Figure S12. Powder X-ray diffraction patterns of the materials reported in Figure 5 of the main text.

(1) Phase Transitions in CsSnCl3 and CsPbBr3 An NMR and NQR Study : Zeitschrift für Naturforschung A https://www.degruyter.com/view/j/zna.1991.46.issue-4/zna-1991-0406/zna-1991-0406.xml (accessed Aug 23, 2019).
(2) Kubicki, D. J.; Prochowicz, D.; Hofstetter, A.; Zakeeruddin, S. M.; Grätzel, M.; Emsley, L. Phase Segregation in Cs-, Rb- and K-Doped Mixed-Cation (MA)x(FA)1–XPbI3 Hybrid Perovskites from Solid-State NMR. *J. Am. Chem. Soc.* **2017**, *139* (40), 14173–14180. https://doi.org/10.1021/jacs.7b07223.
(3) Grutzner, J. B.; Stewart, K. W.; Wasylishen, R. E.; Lumsden, M. D.; Dybowski, C.; Beckmann, P. A. A New Mechanism for Spin−Lattice Relaxation of Heavy Nuclei in the Solid State: 207Pb Relaxation in Lead Nitrate. *J. Am. Chem. Soc.* **2001**, *123* (29), 7094–7100. https://doi.org/10.1021/ja0040924.